

Enhancing PEM Fuel Cell Efficiency with an Integrated Organic Rankine Cycle Using Low-GWP Working Fluids

Bagus Putra Pratama[1] – Reynolds Widhiyanurrochmansyach[1] – Widya Wijayanti[2] – Jayan Sentanuhady[1,✉]

1 Department of Mechanical and Industrial Engineering, Universitas Gadjah Mada, Yogyakarta, Indonesia
2 Department of Mechanical Engineering, Brawijaya University, Malang, Indonesia
✉ jayan@ugm.ac.id

Abstract *Proton exchange membrane fuel cells (PEMFCs) offer high-efficiency, zero-emission electricity, yet 45 % to 60 % of their input chemical energy is lost as low-grade waste heat. In response to this problem, this study presents a thermodynamic analysis of a 50 kW PEMFC thermally integrated with a sub-critical organic Rankine cycle (ORC) to convert this waste heat into additional power. Using a high-fidelity model validated with previous study, this study compares low-global warming potential (GWP) working fluids (R1233zd(E), R1234yf, R1234ze(Z)) against the legacy R245fa under a practical fixed-state-point control strategy. The results demonstrate up to 3 % increase in total electrical efficiency, driven by the successful conversion of the PEMFC's low-grade waste heat into additional net power output by the ORC bottoming cycle. The main novelty of this research lies in the first comprehensive demonstration that a 3 % system efficiency enhancement can be sustainably achieved by integrating low-GWP working fluids and a practical fixed-state-point control strategy to ensure stable operation. The analysis confirms that the thermodynamically limited ~5 % ORC thermal efficiency can be realized without compromising energy recovery potential, proving that the pursuit of sustainability is compatible with enhanced system performance. R1234yf is identified as the superior low-GWP fluid for high-load operations, while R1233zd(E) proves optimal for low-load conditions, validating a robust pathway for designing next-generation, eco-friendly fuel cell systems.*

Keywords *proton exchange membrane fuel cell, organic Rankine cycle, low-global warming potential working fluid, waste-heat recovery*

Highlights

- *A high-fidelity PEMFC-ORC hybrid system model is developed and validated.*
- *System integration increases overall electrical efficiency by up to about 3 %.*
- *Next-generation low-GWP working fluids show excellent performance vs. legacy R245fa.*
- *The research demonstrates that sustainability and high efficiency are simultaneously achievable.*

1 INTRODUCTION

The rising global demand for energy, coupled with serious environmental concerns, has accelerated the advancement of clean energy technologies. Proton exchange membrane fuel cells (PEMFCs) have emerged as a very promising alternative due to their outstanding energy conversion efficiency, compact size, and zero emissions during operation [1]. Recent advancements in the endurance of catalysts and membrane materials have rendered them applicable in various domains, including transportation, decentralized power generation, and portable systems for unmanned aerial vehicles (UAVs) [2].

Despite these advantages, PEMFCs encounter a significant challenge: a considerable portion of the energy input is dissipated as waste heat, resulting in diminished overall system efficiency. If not efficiently recovered, this waste heat constrains the energy utilization of fuel cell devices. Recent research has highlighted the importance of this issue. Generally, approximately 45 % to 60 % of the total input energy in a PEMFC system is lost as heat via the exhaust gas and coolant streams, rendering it a significant inefficiency of the technology [3]. Sophisticated thermal management may improve PEMFC efficiency by as much as 5 %, whereas absorbing waste heat from exhaust or cooling streams could elevate overall system efficiency by up to 10 % [4,5]. These data indicate that waste heat is not only an external problem but an underlying inefficiency in PEMFC operation.

Many researchers are presently investigating the integration of PEMFC and ORC systems. Preliminary modeling tests successfully confirmed the viability of this hybrid arrangement, demonstrating significant enhancements in efficiency. Liu et al. [6] enhanced the overall system efficiency by 5.84 %, whereas Wilberforce and Muhammad [7] developed dynamic models to ensure optimal system performance. An analysis of the present state of the art reveals that these foundational investigations predominantly employed traditional working fluids, such as R134a and R245fa. Due to their elevated global warming potentials (GWPs) of 1430 and 1030, these fluids are currently deemed environmentally outdated. International regulations, such as the Kigali Amendment to the Montreal Protocol, make the use of certain substances unlawful, necessitating a transition to more sustainable alternatives [8].

Concurrently, an alternative research area has been investigating and evaluating low-GWP working fluids for broad ORC applications. Hydrofluoroolefins (HFOs), including R1233zd(E), R1234yf, and R1234ze(Z), are acknowledged as optimal options due to their minimal GWP and exceptional thermodynamic properties. Yang et al. [9] have shown that fluids such as R1233zd(E) perform comparably to or surpass R245fa while exerting a much lower environmental impact. While hydrofluoroolefins (HFOs) offer substantial reductions in direct greenhouse gas emissions due to their very low global warming potential, recent environmental discussions have raised concerns regarding the atmospheric degradation of certain fluorinated refrigerants into persistent byproducts such as trifluoroacetic acid (TFA), which is associated with broader PFAS-related environmental concerns [10]. Although the present study focuses specifically on thermodynamic performance and energy recovery potential, this environmental aspect should be acknowledged and warrants future life-cycle environmental assessment when evaluating refrigerant sustainability comprehensively.

 DOI: 10.5545/sv-jme.2026.1641

Natural refrigerants such as ammonia (NH_3), carbon dioxide (CO_2), hydrocarbons, and water are also recognized as environmentally favorable alternatives due to their negligible GWP and absence of fluorinated degradation concerns. However, the present study intentionally focuses on commercially relevant low-GWP HFO-based working fluids that serve as near-replacement candidates for conventional ORC refrigerants under compact low-temperature PEMFC waste heat conditions. Natural refrigerants often introduce additional challenges related to toxicity, flammability, or significantly different operating pressure requirements, which would require a fundamentally different cycle design framework beyond the scope of the present comparative investigation [11,12].

This analysis reveals a significant research gap: while PEMFC-ORC systems have been modeled with conventional fluids and low-GWP fluids have been assessed for generic ORCs, there is a lack of comprehensive, validated studies that systematically evaluate the performance of next-generation low-GWP HFOs specifically within an integrated PEMFC-ORC framework. Furthermore, the practical implications of implementing a controller-friendly, fixed-state-point operational strategy with these novel fluids have not been adequately investigated.

While previous studies have explored PEMFC-ORC systems, the practical implementation of innovative low-GWP working fluids has been significantly overlooked. This research directly confronts this gap by building a robust analytical framework with three core objectives. The foundation of our work is a high-fidelity numerical model of a 50 kW PEMFC-ORC system, validated with less than 5 % error, which mitigates experimental risks by enabling precise performance predictions. Building upon this model, our study provides the first comprehensive comparative assessment of next-generation low-GWP fluids (R1233zd(E), R1234yf, R1234ze(Z)) versus the conventional R245fa. This analysis extends beyond simple efficiency to critically evaluate net power output and parasitic loads, offering vital insights into their real-world efficacy. To complete the framework, we demonstrate the system's effectiveness under a pragmatic fixed-state-point control strategy, proving that enhanced performance and operational stability can be achieved simultaneously. This integrated approach validates a clear and feasible pathway for designing next-generation, eco-friendly fuel cell systems.

2 METHODS & MATERIALS

2.1 Working Fluid Selection

Four working fluids were selected for comparative analysis. R245fa was chosen as a widely studied legacy refrigerant. Three low-GWP fluids were selected as environmentally compliant alternatives: R1233zd(E), R1234yf, and R1234ze(Z). These fluids were chosen for their favorable thermodynamic properties in low-temperature applications and their alignment with global environmental regulations. Key properties are summarized in Table 1.

2.2 System Operating Parameters and Boundary Conditions

The simulation was performed based on a 50-kW nominal power PEMFC stack. Key operating parameters for the PEMFC and the fixed state-point conditions for the ORC are detailed in Tables 2 and 3. The isentropic efficiencies for the ORC turbine and pump were set to 80 %, while the air compressor efficiency was 85 %. These values were selected based on reported benchmarks for micro-scale ORC systems and auxiliary components of comparable capacity. The ORC was controlled to maintain a nearly constant evaporation temperature (≈50 °C) and condensation temperature (≈27 °C) across all operating loads to ensure stable and controller-friendly operation.

The integrated proton exchange membrane fuel cell–organic Rankine cycle (PEMFC–ORC) system was simulated using a numerical modeling framework implemented through Aspen custom modeler (ACM) and Aspen Plus. These platforms enabled a hybrid

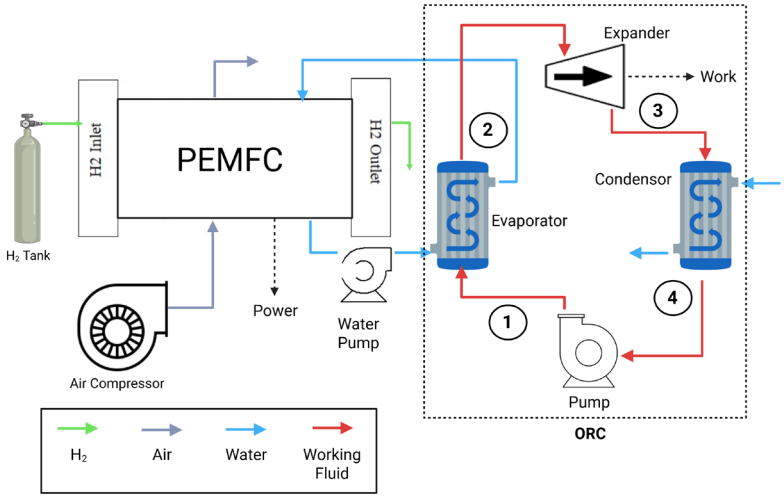

Fig. 1. Illustration of proposed integrated ORC-PEMFC system

Table 1. Thermodynamics property comparison of working fluids [13-17]

Working fluid	Boiling point [°C]	Critical temperature [°C]	Critical pressure [MPa]	GWP [100-yr]	ASHRAE safety class	Flammability
R1234yf	-29.4	94.7	3.38	4	A2L	Mildly flammable
R1234ze	9.47	166.1	3.63	1.4	A2L	Mildly flammable
R1233zd	18.3	165.6	3.62	1	A1	Non-flammable
R245fa	15.3	154	3.65	1030	B1	Non-flammable

equation-oriented and sequential-modular approach, facilitating detailed representation of thermodynamic, electrochemical, and transport processes under varying load conditions.

The simulation of the integrated PEMFC-ORC system was developed using Aspen Plus V14. The modified Benedict-Webb-Rubin, explicit in Helmholtz energy, equation of state with reference fluid properties (REFPROP) was selected as the property method, as it is robust for predicting the thermodynamic properties of both polar and non-polar components, including the organic refrigerants used in this study. Key components of the ORC loop were modeled using standard Aspen Plus blocks: the evaporator and condenser were simulated using heater blocks with specified heat duties derived from the PEMFC waste heat profile, the pump was modeled using a pump block with a defined isentropic efficiency of 80 %, and the turbine was represented by a turbine block with an isentropic efficiency of 80 %. Pressure drops within the heat exchangers were assumed to be negligible to isolate the thermodynamic performance of the working fluids.

Initial model setup involved defining system-level parameters such as the number of PEMFC cells, electrode active area, stoichiometric ratios of reactants, as well as boundary conditions for the ORC. Thermophysical properties for all process streams were derived using Aspen Plus property libraries, notably the modified Benedict-Webb-Rubin equation of state and REFPROP correlations. The simulation leveraged the ability to embed ACM-based modules within Aspen Plus to exploit the benefits of custom equation-oriented modeling inside a sequential-modular simulation environment [18].

The PEMFC subsystem was modeled using a set of electrochemical equations describing voltage-current relationships, reactant consumption rates, and associated overpotentials, including activation, ohmic, and concentration losses. Iterative solving techniques were used to compute cell voltage, current density, and heat rejection. This methodology reflects validated practices for embedding custom fuel cell models within large-scale process flowsheets [18].

The ORC block was developed within Aspen Plus based on energy and mass conservation equations for each component: evaporator, expander, condenser, and pump. Heat rejected from the PEMFC was utilized as the thermal input to the ORC evaporator. Thermodynamic state points were updated iteratively until convergence was achieved, with a residual error tolerance of 10^{-6} for both mass and energy balances. These techniques align with recent ORC simulation studies that evaluated system performance under different operating conditions and working fluids [19].

Coupling between the PEMFC and ORC was facilitated through a data exchange interface that ensured consistency in energy transfer, particularly from the PEMFC coolant stream to the ORC evaporator. The Newton–Raphson method with adaptive step-size control was used to solve the set of nonlinear algebraic equations, a robust solver choice supported in various Aspen-based process simulations [20].

Upon convergence at a given PEMFC load point, the integrated model provided detailed outputs including net electrical efficiency, ORC power recovery, total system exergy, and thermal integration performance. The simulation was repeated across a range of operating conditions to assess overall system behavior and identify performance trends under variable loading. Such simulation methodologies are critical in evaluating integrated energy systems and optimizing thermal recovery strategies.

2.3 System Description

The ORC starts at the pump, where the working fluid exists as a cool, subcooled liquid. From Figure 1, the pump elevates the pressure with minimal energy consumption, preparing for heat to perform the primary work. The fluid, under pressure and in liquid form, enters the evaporator, which serves as the common heat exchanger connecting it to the waste heat of the fuel cell. The heat from the PEMFC's coolant converts the liquid into vapor, typically providing a small degree of superheat to prevent any droplets from persisting in the subsequent travel. The vapor next encounters the expander, be it a micro-turbine, scroll, or screw, where it relinquishes its pressure and temperature as productive shaft work that drives a generator. The expanded low-pressure vapor enters the condenser, dissipates its residual heat to the surrounding air or a cooling-water system, and reverts to a liquid state. The loop is complete when the liquid returns to the pump, establishing a repetitive cycle: pump, evaporator, expander, condenser—each element facilitating a distinct transformation, with each repetition converting low-grade heat into clean power.

Additionally, the PEMFC maintains its own cycle via a controlled cooling loop. Within the stack, a jacket of circulating coolant absorbs reaction heat and exits at a consistent 75 °C, adequate to maintain membrane hydration while remaining cool enough to prevent stress. The heated stream directly enters the evaporator utilized by the ORC, transferring its thermal energy to vaporize the organic fluid. As energy crosses the exchanger, the coolant's temperature decreases towards its target return temperature. Upon reaching the stack inlet, the coolant returns to 50 °C, prepared to absorb heat once more.

2.4 Thermodynamic Modelling of PEMFC & ORC

Before delving into the specific mathematical formulations of the PEMFC, it is essential to establish a broader thermodynamic framework that governs its operation. The performance of a PEMFC is fundamentally dictated by the balance between electrochemical energy conversion and the inherent thermodynamic limitations of the system. In practice, the ideal electrochemical potential predicted by thermodynamics is rarely achieved, as irreversible losses arising from reaction kinetics, ionic and electronic resistances, and mass transport constraints must be accounted for. Consequently, the transition from theoretical energy balances to practical cell voltage requires a detailed consideration of these losses. This necessitates a comprehensive model in which the cell voltage is derived not only from the Nernst potential, which represents the maximum reversible voltage, but also from correction factors that reflect real-world inefficiencies. The following section introduces the PEMFC model equations that capture this interplay, providing the foundation for subsequent integration with the ORC system.

The single-cell voltage of PEMFC is referred to Nernst potential equation. Nernst equation is the ideal voltage from electrochemistry reaction generated by PEMFCs. However, single-cell voltage also needs to consider the irreversible losses in a steady-state PEMFC model, which are activation losses, ohmic losses, and concentration losses. The single-cell voltage value can be written as follows [21]:

$$V_{cell} = E_{nernst} - V_{act} - V_{ohmic} - V_{conc}, \tag{1}$$

where E_{nernst} is known as Nernst potential, V_{act} is activation losses, V_{ohmic} is ohmic losses, and V_{conc} is concentration losses.

Nernst equation can be determined as follows [6]:

$$E = E_0 + \frac{RT_{op}}{nF} ln\left(\frac{P_{H2}P_{O2}^{0.5}}{P_{H2O}}\right), \tag{2}$$

where E_0 is the standard condition (25 °C and 1 bar) of Nernst potential, which is 1.229 V, variable R is the universal gas constant, T_{op} is the operating temperature of PEMFC, n is the number of electrons, F is Faraday constant, and P_{H2}, P_{O2}, and P_{H2O} are partial pressure of hydrogen, oxygen, and water, respectively.

From Equation (2), the partial pressures of the corresponding gases can be described as follows [22]:

$$P_{H2} = \left(0.5P_{H2O}\right)\left[\frac{1}{\exp\left(\frac{1.653i}{T_{op}^{1.334}}\right)x_{H2O}^{sat}} - 1\right], \tag{3}$$

$$P_{O2} = P_{op}\left[1 - x_{H2O}^{sat} - x_{N2}^{channel}\exp\left(\frac{0.291i}{T_{op}^{0.832}}\right)\right], \tag{4}$$

$$x_{H20}^{sat} = \frac{P_{H2O}}{P_{op}}, \tag{5}$$

where i is the current density, $x_{N2}^{channel}$ is the mass fraction of nitrogen, x_{H2O}^{sat} is the mass fraction of water at saturation; T_{op} and t_{op} are the PEMFC operating temperatures in Kelvin and Celsius, respectively.

Additionally, the unknown parameter from Eqs. (3-5), such as P_{H2O} is derived as follows [22]:

$$\log\left(P_{H2O}\right) = -2.1794 + 0.02953t_{op} - 9.1837\times10^{-5}t_{op}^{2} + 1.4454\times10^{-7}t_{op}^{3}. \tag{6}$$

Activation losses are caused by electrode kinetics due to the charge transfer coefficient in PEMFC electrochemical reactions. The value of activation loss can be calculated using the Eq. (7) [6]:

$$V_{act} = \frac{RT}{\alpha F}\ln\left(\frac{i}{i_0}\right), \tag{7}$$

where α and i_0 are transfer coefficient and exchange current density, respectively. Meanwhile, ohmic loss arises from the effect of resistance. Ohmic losses can be expressed as follows:

$$V_{ohmic} = iR_{cell}. \tag{8}$$

where R_{cell} is resistance value of PEMFC. The value of resistance obtained from either experimenting or referring to available research. Typically, this value ranges from 0.5 Ω to 1.5 Ω depending on the electrode material.

Concentration loss is determined by concentration gradient that occurs as the result of reactant consumption. This loss can be expressed as follows [6]:

$$V_{conc} = \frac{RT}{nF}\ln\left(\frac{i_L}{i_L - i}\right). \tag{9}$$

Thus, power generation of PEMFC is simply the product of the current and the generated cell voltage. Specifically, power of PEMFC can be valued by the calculation of the Eq. (10) [22]:

$$W_{stack} = N_{cell}E_{cell}iA, \tag{10}$$

where W_{stack} is the power generated in PEMFC, and A is cross section area of PEMFC electrode. Assuming air behaves as an ideal gas, isentropic compression in an air compressor is determined using Eq. (11) [23]:

$$\frac{T_{out,s}}{T_{amb}} = \pi^{\left(\frac{k-1}{k}\right)}, \tag{11}$$

where k denotes the isentropic exponent, π signifies the pressure ratio, $T_{out,s}$ refers to the outlet temperature of the isentropic process, and T_{amb} indicates the ambient temperature. Simultaneously, the isentropic efficiency of the compressor is represented by Eq. (12) [23]:

$$\eta_{comp} = \frac{T_{out,s} - T_{amb}}{T_{out,comp} - T_{amb}}, \tag{12}$$

where, $T_{out,comp}$ represents the actual air temperature at the compressor exit. Consequently, the power required for the compressor is determined using Eq. (13) [23]:

$$W_{comp} = \frac{\dot{m}_{air}\left(\frac{k}{k-1}\right)RT_{amb}\left(\pi^{\frac{k-1}{k}} - 1\right)}{\eta_{comp}}, \tag{13}$$

where, $\dot{m}_{air}$ denotes the mass flow rate of air.

2.4.1 Heat Losses of PEMFC

The energy source in an operational fuel cell is the electrochemical reaction. Nevertheless, a significant portion of energy is lost as heat, over 50 % under nominal conditions. Excess thermal energy must be dissipated from the fuel cell to prevent overheating. Net thermal energy can be determined using the thermodynamic energy balance within the cell as follows:

$$Q_{loss} = Q_{ch} - W_{stack} - Q_{s,l}, \tag{14}$$

where Q_{loss} represents net heat energy, Q_{ch} denotes chemical energy, and $Q_{s,l}$ refers to sensible and latent heat.

The theoretical power provided to the fuel cell stack is directly influenced by the amount of hydrogen used. In a fuel cell, the rates of hydrogen consumption, oxygen consumption, and water production are determined using the stack current and the number of cells as follows [24]:

$$\dot{n}_{H2,cons} = N_{cell}\frac{I}{2F}, \tag{15}$$

$$\dot{n}_{O2,cons} = N_{cell}\frac{I}{4F}, \tag{16}$$

$$\dot{n}_{H2O,gen} = N_{cell}\frac{I}{2F}, \tag{17}$$

where $\dot{n}_{H2,cons}$, $\dot{n}_{O2,cons}$, $\dot{n}_{H2O,gen}$ are hydrogen and oxygen consumption, as well as water generation in electrochemical reaction, N_{cell} is number of cells in PEMFC.

The reactant flow rate at the fuel cell input must equal or exceed the consumption rate of the reactant to prevent membrane degradation and failure in the fuel cell. The stoichiometric rate is employed to resolve this issue; the molar flow rate of the reactant can be determined by [24]:

$$\dot{n}_{H2,cons} = \lambda_{H2}N_{cell}\frac{I}{2F}, \tag{18}$$

$$\dot{n}_{O2,cons} = \lambda_{O2}N_{cell}\frac{I}{4F}, \tag{19}$$

$$\dot{n}_{H2O,gen} = N_{cell}\frac{I}{2F}, \tag{20}$$

where λ_{H2} and λ_{O2} are stoichiometric rate of hydrogen and oxygen, respectively. The theoretical power generated from an electrochemical process is expressed as [24]:

$$Q_{ch} = \dot{n}_{H2,cons}HHV, \tag{21}$$

where HHV represents the higher heating value of hydrogen. The sensible and latent heat can be calculated by [6]:

$$Q_{s,l} = C_{H2}\left(\dot{n}_{H2,\,out}T_{op} - \dot{n}_{H2,in}T_{amb}\right) + C_{O2}\left(\dot{n}_{O2,\,out}T_{op} - \dot{n}_{O2,in}T_{out,comp}\right) + C_{N2}\left(\dot{n}_{N2,out}T_{op} - \dot{n}_{N2,in}T_{out,comp}\right) + \dot{n}_{H2O,gen}\left(T_{op} - T_{amb}\right)C_{H2O} + \dot{n}_{H2O,gen}H_v, \quad (22)$$

where C_{H2}, C_{O2}, C_{N2}, C_{H2O} are the specific heat capacity of hydrogen, oxygen, nitrogen and water respectively, Hv represents the vaporization heat of water.

2.4.2 ORC Equation Modelling

ORC analysis generally uses a T-s diagram as its basis. The analysis involves calculating the power or thermal output from each operation component, including the pump, evaporator, condenser, and turbine. The working fluid exists in four different states, as denoted by the numbers in Fig. 2.

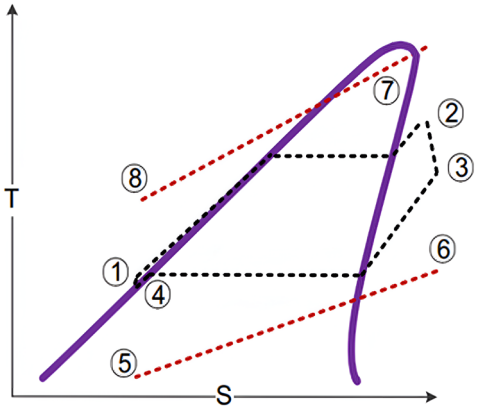

Fig. 2. Typical T-s diagram of ORC system

Evaporator captures the heat rejected from PEMFC to evaporate working fluid of ORC. The value of transferred heat can be calculated by [23]:

$$\dot{Q}_{evap} = \dot{m}_{ORC}\left(h_2 - h_{1,a}\right). \quad (23)$$

Like evaporator, the heat rejected to environment from condenser is determined as follows [23]:

$$\dot{Q}_{cond} = \dot{m}_{ORC}\left(h_{3,a} - h_4\right). \quad (24)$$

For the moving parts, specifically the pump and turbine, the power required by the pump and generated by the turbine, respectively, in the ORC system is calculated by [23]:

$$\dot{W}_{ORC} = \dot{m}_{ORC}\left(h_2 - h_{3,a}\right). \quad (25)$$

Because the moving parts in the ORC have isentropic efficiency, the value of enthalpy in pump and turbine shifted accordingly from isentropic condition to real condition, calculated by these equations, respectively [23]:

$$\eta_{pump} = \frac{h_{1,s} - h_4}{h_{1,a} - h_4}, \quad (26)$$

$$\eta_{turbine} = \frac{h_2 - h_{3,a}}{h_2 - h_{3,s}}, \quad (27)$$

where h is the specific enthalpy of each state.

2.4.3 Performance Evaluation of ORC-PEMFC Integration

The performance of the proposed hybrid power system may be assessed by the thermal efficiency of the ORC system, the electrical efficiency of the proton exchange membrane (PEM) fuel cell, and the overall electrical efficiency. Then, the efficiency of th ORC is calculated as follows [6]:

$$\eta_{ORC} = \frac{\dot{W}_{ORC} - \dot{W}_{pump}}{\dot{Q}_{evap}} \times 100\,\%. \quad (28)$$

The PEM fuel cell electrical efficiency is calculated as follows:

$$\eta_{PEMFC} = \frac{\dot{W}_{PEMFC} - \dot{W}_{comp}}{\dot{Q}_{ch}} \times 100\,\%. \quad (29)$$

The overall electrical efficiency is calculated by [6]:

$$\eta_{eff} = \frac{\dot{W}_{PEMFC} + \dot{W}_{ORC} - \dot{W}_{pump} - \dot{W}_{comp}}{\dot{Q}_{ch}}. \quad (30)$$

2.5 Variable Conditions of Hybrid System

In this paper, there are several PEMFC operating conditions that are either known or determined by the author, as shown in Table 2. PEMFC is designed to produce 50 kW of nominal power.

Table 2. Operating parameter of PEMFC

Symbol	Name of parameter	Value
N_{cell}	Number of cells	220
A	Active cell area	50 A cm^{-2}
T_{op}	Operating temperature	75 °C
T_{amb}	Ambient temperature	25 °C
P_{op}	Operating pressure	1.5 bar
i_o	Exchange current density	3.10^{-6} A cm^{-2}
R	Ohmic area-specific resistance	0.5 Ω
i_L	Limiting current density	1.2 A cm^{-2}
α	Transfer coefficient	0.5
F	Faraday number	96,485 C mol^{-1}
R	Universal gas constant	8.314 J mol^{-1} K^{-1}
λ_{air}	Stoichiometric rate of air	2
λ_{H2}	Stoichiometric rate of hydrogen	1.2
$C_{p,H2}$	Specific heat capacity of hydrogen	28.86 J mol^{-1} K^{-1}
$C_{p,O2}$	Specific heat capacity of oxygen	29.72 J mol^{-1} K^{-1}
$C_{p,N2}$	Specific heat capacity of nitrogen	29.13 J mol^{-1} K^{-1}
$C_{p,H2O}$	Specific heat capacity of water	75.95 J mol^{-1} K^{-1}
H_v	Vaporization heat of water	40,644 J mol^{-1}
HHV	Higher heating value of hydrogen	285.55 kJ mol^{-1} K^{-1}
k	Isentropic exponent	1.4
π	Pressure ratio	1.5
η_{turb}	Turbine isentropic efficiency	80 %
η_{pump}	Pump isentropic efficiency	80 %
η_{comp}	Air compressor isentropic efficiency	85 %

The designed ORC system was evaluated under a fixed-state-point operating strategy, in which evaporation and condensation temperatures were maintained at approximately 50 °C and 27 °C, respectively, for all working fluids. This assumption was intentionally adopted to establish a controlled comparative framework for evaluating working-fluid performance under identical thermodynamic boundary conditions.

In practical implementation, maintaining these target temperatures would be achieved through operational control variables such as working-fluid mass flow adjustment, condenser cooling-water flow regulation, and heat-exchanger thermal management. As PEMFC load increases and greater waste heat becomes available, the ORC working-fluid circulation rate would be correspondingly adjusted to preserve the intended evaporator operating condition. Therefore,

the present strategy represents a controller-friendly comparative thermodynamic assumption rather than full dynamic control implementation. The ORC system parameters are stated in Table 3.

Table 3. Working fluid operating conditions of ORC

Working fluid	State	T [°C]	P [bar]	H [kJ kg^{-1}]	s [kJ kg^{-1} K^{-1}]
R1233zd	1	27.2	2.8	-192.022	-0.6565
	2	50	2.8	14.166	-0.013
	3	34.1	1.4	3.84	-0.004
	4	27	1.4	-191.883	-0.657
R1234yf	1	27.4	12.8	-1118.09	-2.613
	2	50	12.8	-962.335	-2.127
	3	31.03	7.2	-970.552	-2.119
	4	27	7.2	-1118.733	-2.614
R1234ze	1	27.36	9.8	-7211.08	-2.567
	2	50	9.8	-7032.4	-2.009
	3	31.49	5.3	-7041.82	-2.002
	4	27	5.3	-7231.56	-2.567
R245fa	1	27.1	3.4	-8950.34	-4.294
	2	50	3.4	-8743.38	-3.65
	3	33.8	1.6	-8754.23	-3.64
	4	27	1.6	-8950.51	-4.294

To systematically compare the suitability of low-global warming potential (GWP) refrigerants for high-efficiency thermal systems, we conducted a comprehensive evaluation of four candidate fluids: R1234yf, R1234ze(Z), R1233zd(E), and R245fa. These refrigerants were selected based on their relevance in recent refrigeration, air conditioning, and ORC applications. The analysis integrates both thermodynamic parameters, such as boiling point, critical temperature, and pressure, and safety metrics defined by ASHRAE, including toxicity and flammability classifications from Table 1.

3 RESULTS AND DISCUSSION

The main findings from the thoroughly evaluated numerical simulation methodology are presented. The analysis proceeds by ensuring the model's accuracy through a comprehensive comparison with available data. The next section presents the performance of the integrated hybrid system, highlighting the overall efficiency improvements and providing a comprehensive comparison of the selected low-GWP working fluids. The conclusion includes an explanation that elucidates these findings, situates them within the framework of current research, and specifically highlights the novel and significant aspects of this study.

3.1 ORC Behavior under Coupled Waste Heat Input

The ORC's operation is tightly linked to the magnitude of waste heat transferred from the PEMFC coolant loop. With fixed thermodynamic state points (evaporation at ~50 °C and condensation at ~27 °C), the enthalpy differences across each ORC component remain constant, leading to a cycle efficiency that is largely invariant with respect to PEMFC load.

The implication is a clean separation of "quality" and "quantity": the cycle's quality (efficiency) stays stable, while its quantity (net power) increases with fuel-cell current. For applications where predictability and controller simplicity are priorities, fixed state points offer a robust baseline from which more advanced, off-design strategies (e.g., sliding pressure, variable superheat) can later be explored if marginal efficiency gains are worth the added complexity.

Because efficiency remains approximately constant by design, net ORC power grows with PEMFC current as shown in Fig. 3. Yet the ordering of fluids by net power is not guaranteed to match the ordering by efficiency. In the results, small efficiency differences across candidates translate into subtly different net-power outcomes once mass-flow scaling and pump work are accounted for. At high load, R1234yf can deliver the largest net watts even though its efficiency is not the highest, while R245fa, often the efficiency leader, tracks closely behind.

This divergence underscores a key design lesson: when evaluating bottoming cycles in compact systems with modest temperature lifts, ranking by efficiency alone can mislead. The metric that matters to the bus bar (net watts) is shaped by both turbine work and auxiliary consumption. Consequently, fluid choices should be judged in the specific control framework and load range in which the system will operate.

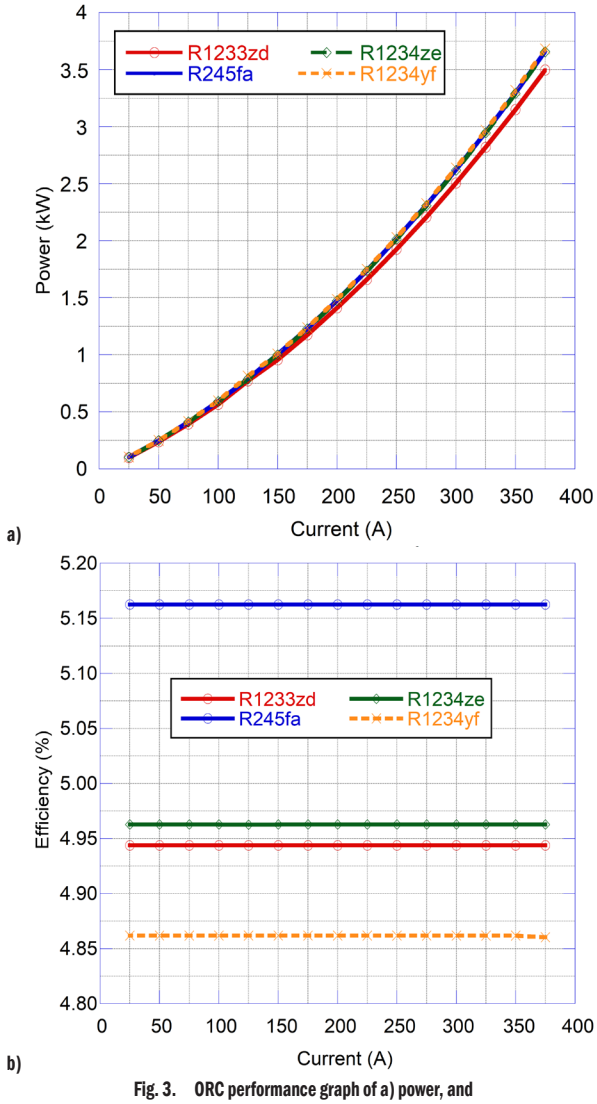

Fig. 3. ORC performance graph of a) power, and b) efficiency with variation of current and working fluid

Auxiliary work, especially pump power as shown in the Fig. 4a, acts as a performance hinge in low-to-moderate temperature ORCs. In your comparison, R1234ze consistently incurs the highest

pumping penalty, whereas R1233zd and R245fa impose the lowest, with R1234yf in between. These penalties matter because they subtract directly from turbine output; two fluids with similar turbine work can yield different net power purely due to pump demands.

Mass-flow behavior complements this picture, as shown in Fig. 5. As fuel-cell load rises and more heat becomes available, all fluids require higher circulation rates, but not equally so. Differences in thermo-physical properties (density, viscosity, saturation slope, latent heat) mean that some fluids achieve the same thermal lift at lower flow, easing both pump sizing and parasitic consumption. Designers targeting compact hardware or limited auxiliary power budgets should therefore weigh pumping economy on par with headline cycle efficiency.

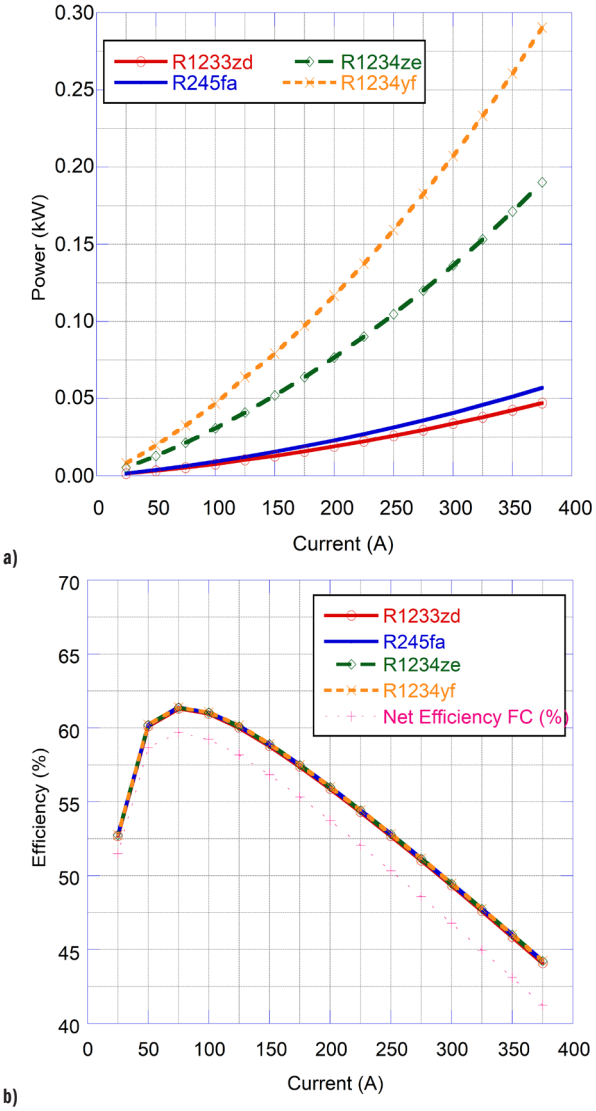

Fig. 4. Performance graph of a) pump power required for ORC and b) overall efficiency of ORC-PEMFC with variations of working fluid vs current density

3.2 Comparative Analysis of Working Fluid

Previous part implies that the decision of working fluid critically determines the balance between efficiency, auxiliary requirements, and environmental sustainability. Four fluids were compared: the conventional R245fa and three low-GWP alternatives—R1233zd(E), R1234yf, and R1234ze(Z).

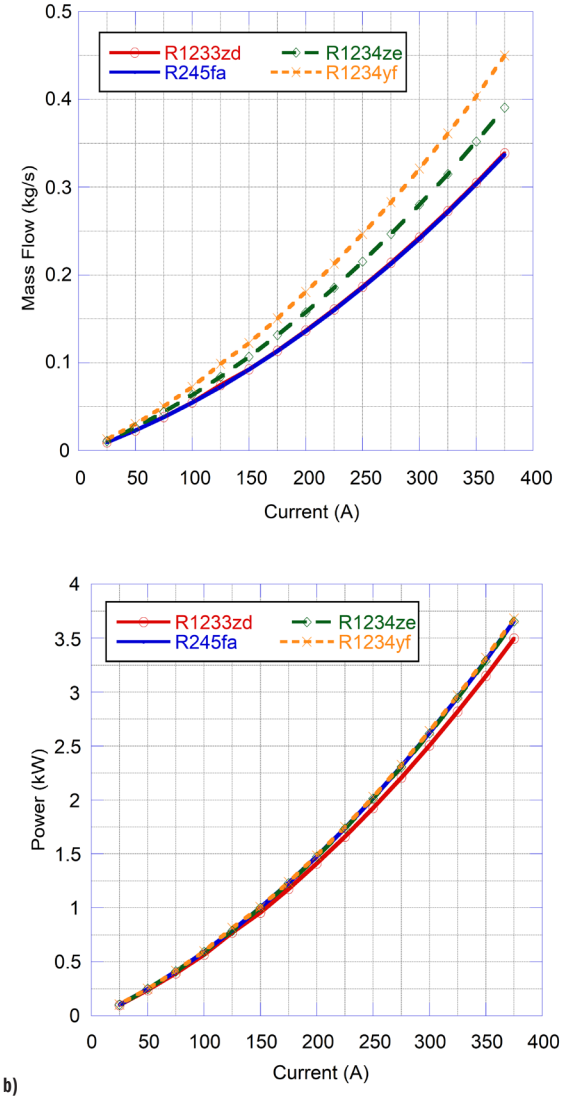

Fig. 5. Mass flow behavior of: a) working fluid, and b) cooling water used in the ORC condenser vs current

The present study offers a comprehensive improvement over existing literature by integrating net power output, thermodynamic efficiency, auxiliary energy consumption, and mass flow behavior into a unified framework for working fluid selection in PEMFC–ORC systems. While Moon et al. [25] evaluated low-GWP fluids such as R1234yf and R1233zd(E) primarily on the basis of turbine performance within ocean thermal energy conversion, this study extends the analysis by incorporating auxiliary power demands and system-level net power. It was found that R1234yf, although not the most efficient thermodynamically, delivered the highest net power at elevated PEMFC current densities due to its advantageous enthalpy characteristics and favorable expansion behavior.

Furthermore, although Icaranom et al. [26] demonstrated that R1233zd(E) mixtures closely approach the efficiency of R245fa, they did not quantify real-world auxiliary energy impacts. This study improves upon those findings by demonstrating that R1233zd(E) maintains competitive cycle efficiency with significantly lower pumping penalties, enhancing its viability as a sustainable replacement. In addition, while Witanowski [27] emphasized compressor performance and COP in ORC-VCC systems, the current work highlights that R1234ze(Z), despite acceptable cycle efficiency, suffers from the highest auxiliary power burden due to

Table 4. ORC system model validation [6,23,29]

Parameter	Liu et al. [6]	Lu et al. [23]	Bull et al. [29]	Current study	Deviation [%]	Remarks
ORC thermal efficiency (η_{ORC}) [%]	10.8	10.5	3 to 6	4.0 to 5.3	–52 % vs. [23]	Matches low-temperature ORC regime [29]; lower due to 75 °C source
Total hybrid efficiency (η_{total}) [%]	54.0 %	53.8 %	—	45.9 to 61.3	≤ 1.5 % vs. [6] and [23]	Confirms consistency of hybrid system thermodynamics
Operating temperature range [°C]	90 to 110	80 to 100	< 80	75	—	Current study operates at lower T regime; aligns with [29]

increased pump demand—resulting in diminished net output. Finally, building on insights by Park et al. [28], who reported that high-latent-heat fluids reduce refrigerant mass flow in automotive systems, this study demonstrates that R1233zd(E)'s elevated latent heat reduces the required circulation rate within the ORC. This characteristic contributes to reduced parasitic losses, smaller pump sizing, and improved mechanical efficiency, underscoring the importance of fluid thermophysical properties in compact energy systems.

3.3 Model Validation

To ensure the credibility and robustness of the hybrid PEMFC–ORC simulation framework, the model was rigorously validated against published numerical and experimental data from recent literature. The validation, summarized in Tables 4 and 5, encompasses both subsystems independently, benchmarking key thermodynamic and electrochemical metrics to assess overall model fidelity.

Table 5. PEMFC system model validation [6,23,30,31]

Parameter	Proposed model	Reference value	Source
Max power	53.29 kW	50.1 kW	[6]
Voltage at 1 A/cm²	0.62 V	0.645 V	[31]
Efficiency at 0.8 A/cm²	50.41 %	54 %	[23]
Internal resistance	0.0801 Ω cm²	0.0725 Ω cm²	[30]

For the PEMFC subsystem, the semi-empirical electrochemical formulation used in this study was benchmarked against previously validated PEMFC models employing comparable Nernst potential, activation, ohmic, and concentration loss formulations [15,16]. The predicted trends in cell voltage reduction with increasing current density and corresponding waste heat generation were found to be consistent with published results.

For the ORC subsystem, validation was performed by comparing thermodynamic behavior—including net power trends, efficiency range, and working-fluid response—with published low-temperature ORC studies under similar operating conditions [29]. The obtained ORC thermal efficiencies (~4.8 % to 5.2 %) and power recovery trends were found to be within expected ranges for low-grade heat recovery applications operating below 80 °C.

Since the primary objective of this work is comparative assessment of working-fluid suitability under identical boundary conditions rather than exact replication of a specific experimental setup, agreement with validated literature behavior is considered sufficient to establish model credibility.

As detailed in Table 4, the thermal performance of the ORC subsystem was benchmarked against data from [6,23,29], each representing validated low- to medium-temperature ORC designs. The model predicts an ORC thermal efficiency of 4 % to 5.3 %, which aligns closely with the reported low-temperature ranges of 3 % to 6 % from [29]. This validates the thermodynamic coherence of the model, especially under low-grade heat source conditions near 75 °C.

Moreover, the model estimates the total hybrid efficiency of the integrated PEMFC–ORC system between 45.9 % and 61.3 %, which deviates by no more than 1.5 % from the reported values of [6,23]. This strong agreement not only confirms the subsystem-level accuracy but also validates the thermal coupling between the fuel cell and ORC stages. The operating temperature range used in this model (~70 °C) further supports its intended application in low-temperature environments, a configuration consistent with the thermodynamic assumptions in [29].

The electrochemical accuracy of the PEMFC model is summarized in Table 5. Key performance indicators such as stack voltage, maximum power output, and internal resistance were benchmarked against authoritative sources. The predicted voltage at 1 A cm^{-2} is 0.62 V, which deviates by less than ~4 % from the 0.645 V reported by) [31], indicating accurate modeling of activation and ohmic overpotentials. Likewise, the predicted maximum power output of 53.29 kW closely matches the 50.1 kW benchmark [6], reflecting high-fidelity prediction across operating loads.

Critically, the model's estimation of internal resistance 0.0801 Ω cm^2 is in near agreement with the experimentally determined value of 0.0725 Ω cm^2 in [30]. This confirms that the model accurately captures both the ionic transport resistance in the membrane and contact resistances across cell components. The calculated efficiency at 0.8 A cm^{-2} stands at 50.41 %, well aligned with the 54 % reference, further validating the electrochemical energy conversion accuracy.

Together, the validation of both subsystems substantiates the model's predictive accuracy for both electrical and thermal outputs. The model is considered sufficiently reliable for the intended system-level analysis. More importantly, the agreement confirms that the heat rejection from the PEMFC, serving as the sole energy input to the ORC, is correctly captured, enabling reliable simulation of hybrid performance under varying working fluid and load conditions. This comprehensive validation underpins the model's use for subsequent performance analysis of novel low-GWP ORC working fluids.

3.4 Synergetic Interaction of ORC and PEMFC

The integration of PEMFCs with ORCs represents a structured opportunity to reclaim and valorize the substantial thermal losses traditionally associated with electrochemical power generation. This study frames the synergistic potential of PEMFC–ORC coupling by proceeding from thermodynamic fundamentals to system-level implementation and sustainability outcomes. It advances beyond earlier analyses by explicitly quantifying the role of dynamic thermal coupling, fluid selection, and fixed state-point control in shaping overall efficiency and net power gains.

At the core of this synergy lies a fundamental thermodynamic mismatch: while PEMFCs offer high electrochemical efficiency and zero-emission operation, they unavoidably release 45 % to 60 % of their input energy as low-grade heat through coolant flows and exhaust gases. This inefficiency, rather than being a design limitation, becomes a latent asset when recontextualized within a hybridized system. By coupling an ORC to the PEMFC, this residual thermal energy can be reclaimed and converted into secondary electrical power, substantially improving energy utilization. Unlike high-temperature solid oxide fuel cells, which pair naturally with steam cycles, PEMFCs operate in a moderate thermal range (typically 60 °C to 80 °C), too low for water-based Rankine systems but ideal for ORCs utilizing low-boiling-point fluids such as R1233zd(E), R1234yf, and R1234ze(Z).

This thermodynamic complementarity enables near-seamless integration. The typical coolant outlet temperature of 75 °C from the PEMFC provides sufficient enthalpy to vaporize these organic working fluids, which possess critical temperatures and saturation characteristics aligned with low-temperature heat sources. In doing so, the ORC not only captures waste energy but also functions as a passive thermal sink, reducing the cooling burden on the PEMFC. This bidirectional benefit stabilizes membrane hydration and maintains stack integrity, while simultaneously delivering scalable electrical output from the ORC expander.

The physical realization of this synergy is achieved via heat exchanger coupling, most often a shell-and-tube ORC evaporator, wherein the PEMFC coolant stream transfers heat to the organic fluid before being recirculated at a controlled inlet temperature. By adopting fixed ORC state points (e.g., evaporation at ~50 °C, condensation at ~27 °C), the hybrid system ensures predictability in performance and avoids the complexity of sliding-pressure or variable superheat control schemes. This approach contrasts with conventional thermoelectric or absorption systems, which either offer minimal efficiency (<5 %) or deliver non-electrical services such as cooling. Compared to these alternatives, the ORC stands out for its compatibility with low-temperature sources, scalability across kilowatt to megawatt levels, and low-GWP refrigerants.

The observed overall efficiency gain of up to 3% is a direct consequence of the fundamental thermodynamic constraints of the system. At nominal load, the PEMFC with approximately 50 % electrical efficiency dissipates about 50 kW of low-grade waste heat. Given the low-temperature nature of this heat source (~75 °C), the ORC's thermal efficiency is thermodynamically limited to approximately 5%, as confirmed by our results (Fig. 4b). Consequently, the maximum recoverable power is around 3.9 kW, which corresponds to a 3 % absolute efficiency gain relative to the 122 kW total fuel energy input. The significance of this finding, and the core novelty of this work, is the quantitative proof from our validated model that this substantial efficiency improvement is fully achievable even when transitioning to environmentally benign, low-GWP working fluids under a practical, fixed-state-point control strategy. This confirms that the pursuit of sustainability does not necessitate a compromise in energy recovery potential for PEMFC systems.

Moreover, as PEMFC current density increases, both waste heat and ORC power output scale proportionally, establishing a natural load-following behavior that enhances energy recovery without necessitating complex real-time control.

Notably, the degree of synergy is not uniform across working fluids. R1234yf exhibited the strongest synergy at high PEMFC loads due to its high vapor expansion potential, yielding the highest net power despite having only moderate cycle efficiency. R1233zd(E) demonstrated a balanced profile with low auxiliary demands and thermal performance close to the traditional, but high-GWP, R245fa, thereby emerging as a sustainable alternative with minimal performance trade-offs. Conversely, R1234ze(Z) incurred the highest pumping penalties, which undermined its net power output even though its vaporization behavior was satisfactory. These results affirm that thermodynamic synergy depends not just on heat source compatibility but also on fluid-specific properties such as latent heat, viscosity, and saturation slope.

The present work advances the field beyond prior studies by combining fluid-specific thermal matching with operational scalability and environmental compatibility. For instance, Witanowski [27] conducted a multi-objective optimization of low-GWP refrigerants for small-scale ORCs, but the study focused primarily on COP and cooling duty without exploring the energy integration dynamics relevant to fuel cells. Salhi et al. [32] examined regenerative ORC configurations and fluid comparisons, yet their findings lacked application specificity to PEMFC temperature ranges or the operational simplicity offered by fixed-point strategies.

A recent study analyzed hybrid PEMFC–ORC systems using zeotropic fluid mixtures, demonstrating high exergy efficiencies but relying on refrigerants with poor environmental performance such as R11–R123 [33]. This study addresses the shortcoming by evaluating fluids like R1233zd(E) and R1234yf, which deliver both technical and regulatory advantages. In parallel, Fan et al. [34] recently proposed a PEMFC–CHP system using phase-change heat pumps for improved thermal recovery. While this approach improved heating efficiency, it diverted heat from electrical augmentation—unlike the present ORC approach, which enhances net power without compromising thermal stability. Similarly, Ngangué et al. [35] optimized ORC–VCC–VAC hybrids using NH_3-based fluids for tropical heat recovery, but their system was oriented toward cooling applications rather than compact power recovery from electrochemical systems. Next, unlike Di and He [36], who optimized cell count in PEMFC–ORC coupling without considering fluid choice, this study shows how thermophysical fluid properties influence not only energy recovery but also component sizing and parasitic demands. Finally, the integration of thermal, mechanical, and environmental considerations into a unified design framework represents a new holistic standard for hybrid system analysis.

Finally, integration brings operational benefits beyond thermodynamic gains. Fixed-state-point operation ensures that ORC efficiency remains stable across PEMFC loads, allowing system designers to sidestep advanced control algorithms. The ORC mass flow rate becomes a direct function of waste heat availability, enabling scalable, predictable behavior well-suited for mobile or decentralized applications. Perhaps most importantly, the combined system enhances environmental sustainability by using zero-emission hydrogen at the fuel cell level and climate-compliant refrigerants at the bottoming cycle. This dual alignment supports regulatory compliance and lifecycle decarbonization, establishing a blueprint for next-generation hybrid power systems that are efficient, robust, and climate-resilient.

3.5 Practical Implementation Considerations

Although the present work focuses on thermodynamic performance comparison, practical implementation aspects are also important for real-world deployment. Low-GWP HFO refrigerants such as R1233zd(E), R1234yf, and R1234ze(Z) are increasingly commercially available due to global regulatory transition away from high-GWP refrigerants. However, these fluids may currently exhibit higher acquisition costs compared to legacy refrigerants such as R245fa, depending on regional market maturity.

Material compatibility must also be considered, particularly regarding seals, lubricants, and expander materials, although several HFO refrigerants have already demonstrated compatibility in modern refrigeration and ORC applications. In addition, mildly flammable classifications (A2L) for R1234yf and R1234ze(Z) require appropriate safety design consideration. These practical constraints do not invalidate their thermodynamic suitability but should be addressed during engineering implementation and techno-economic optimization.

4 CONCLUSIONS

This study successfully developed and validated a high-fidelity numerical model of a 50 kW PEMFC-ORC hybrid system, providing a comprehensive thermodynamic analysis of its performance with next-generation low-GWP working fluids. The key findings are as follows:

1. Integrating an ORC consistently improves PEMFC system efficiency by up to 3 % by converting low-grade waste heat into electricity. This gain aligns with fundamental thermodynamic limits, where the ORC achieves ~5 % thermal efficiency. The core finding from our validated model is that this substantial improvement is fully achievable using new, environmentally benign low-GWP fluids under a practical control strategy. This work confirms that pursuing sustainability does not require compromising the energy recovery potential in advanced fuel cell systems.
2. The comparative analysis demonstrated that modern low-GWP working fluids can match or even exceed the performance of the legacy refrigerant R245fa. R1234yf emerged as the most promising candidate for high-load operations, delivering the highest net power output. Conversely, R1233zd(E) proved to be a well-balanced choice for low-load conditions, offering a near-zero GWP and minimal parasitic losses.
3. The implementation of a fixed-state-point control strategy showed that the ORC's thermodynamic efficiency can be maintained at a stable level regardless of the PEMFC's load. This simplifies the system's control requirements and ensures reliable, predictable operation, which is critical for commercial and mobile applications.
4. This study fills a critical gap in the literature by systematically evaluating low-GWP HFOs within a validated, integrated PEMFC-ORC framework. The results not only provide essential performance benchmarks but also offer a practical roadmap for designing the next generation of efficient, reliable, and environmentally friendly hybrid power systems, in alignment with stringent global climate policies.

Nomenclature

N_{cell}	number of cells, [-]
A	active cell area, [cm^2]
T	temperature [K]
T_{op}	operating temperature, [K]
t_{op}	operating temperature, [°C]
T_{amb}	ambient temperature, [K]
$T_{out,s}$	outlet temperature of isentropic process in compressor, [K]
$T_{out,comp}$	actual outlet temperature in compressor, [K]
P	pressure [bar]
P_{op}	operating pressure, [bar]
P_{H2}	partial pressure of hydrogen, [bar]
P_{O2}	partial pressure of oxygen, [bar]
P_{H2O}	partial fraction of water, [bar]
V_{cell}	single cell voltage, [V]
V_{act}	activation losses, [V]
V_{ohmic}	ohmic losses, [V]
V_{conc}	concentration losses, [V]
E_{nernst}	Nernst potential, [V]
E_0	standard condition Nernst potential, [V]
$\dot{m}_{air}$	mass flow of air in compressor, [kg/s]
x^{sat}_{H2O}	water mass fraction at saturation, [-]
$x^{channel}_{\mathrm{N2}}$	nitrogen mass fraction, [-]
$\dot{n}_{\mathrm{H2},cons}$	hydrogen consumption in PEMFC, [mol/s]
$\dot{n}_{\mathrm{H2},out}$	molar flow of hydrogen in PEMFC outlet, [mol/s]
$\dot{n}_{\mathrm{H2},in}$	molar flow of hydrogen in PEMFC inlet, [mol/s]
$\dot{n}_{\mathrm{O2},cons}$	oxygen consumption in PEMFC, [mol/s]
$\dot{n}_{\mathrm{O2},out}$	molar flow of oxygen in PEMFC outlet, [mol/s]
$\dot{n}_{\mathrm{O2},in}$	molar flow of oxygen in PEMFC inlet, [mol/s]
$\dot{n}_{\mathrm{H2O},gen}$	water generated in PEMFC, [mol/s]
i	cell current density [A cm^{-2}]
i_o	exchange current density, [A cm^{-2}]
i_L	limiting current density, [A cm^{-2}]
α	transfer coefficient, [-]
F	Faraday number, [C mol−1]
R	universal gas constant, [J mol^{-1} K^{-1}]
λ_{air}	stoichiometric rate of air, [-]
λ_{H2}	stoichiometric rate of hydrogen, [-]
$C_{p,\mathrm{H2}}$	specific heat capacity of hydrogen, [J mol^{-1} K^{-1}]
$C_{p,\mathrm{O2}}$	specific heat capacity of oxygen, [J mol^{-1} K^{-1}]
$C_{p,\mathrm{N2}}$	specific heat capacity of nitrogen, [J mol^{-1} K^{-1}]
$C_{p,\mathrm{H2O}}$	specific heat capacity of water, [J mol^{-1} K^{-1}]
H_v	vaporization heat of water, [J mol^{-1}]
HHV	higher heating value of hydrogen, [kJ mol^{-1}]
k	isentropic exponent, [-]
π	pressure ratio, [-]
H	enthalpy [kJ]
s	entropy of the working fluid [kJ kg^{-1} K^{-1}]
η_{ORC}	organic Rankine cycle efficiency, [-]
η_{turb}	turbine isentropic efficiency, [-]
η_{pump}	pump isentropic efficiency, [-]
η_{comp}	air compressor isentropic efficiency, [-]
W_{stack}	power generated in PEMFC, [kW]
Q_{loss}	net energy heat loss of PEMFC, [kW]
Q_{ch}	chemical energy of electrochemical reaction, [kW]
$Q_{s,l}$	sensible and latent heat of PEMFC gases, [kW]

References

[1] Wang, Z., Liu, Z., Fan, L., Du, Q., Jiao, K. Application progress of small-scale proton exchange membrane fuel cell. *Energy Reviews 2* 100017 (2023) **DOI:10.1016/j.enrev.2023.100017**.

[2] Kiani, M., Zhao, Y., Zhang, R. Proton exchange membrane fuel cells: recent developments and future perspectives. *Chem Comm 61* 9392-9411 (2025) **DOI:10.1039/D5CC01478F**.

[3] Lan, Y., Lu, J., Mu, L., Wang, S., Zhai, H. Waste heat recovery from exhausted gas of a proton exchange membrane fuel cell to produce hydrogen using thermoelectric generator. *Appl Energy 334* 120687 (2023) **DOI:10.1016/j.apenergy.2023.120687**.

[4] Wu, Q., Dong, Z., Zhang, X., Zhang, C., Iqbal, A., Chen, J. Towards more efficient PEM fuel cells through advanced thermal management: From mechanisms to applications. *Sustainability 17* 943 (2025) **DOI:10.3390/su17030943**.

[5] Etghani, M.M., Sadripour, S. Evaluation of different scenarios for waste heat recovery in proton exchange membrane fuel cells from energy, environmental, and economic aspects. *Iran J Energy Envir 16* 540-54 (2025) **DOI:10.5829/ijee.2025.16.03.14**.

[6] Liu, G., Qin, Y., Wang, J., Liu, C., Yin, Y., Zhao, J., et al. Thermodynamic modeling and analysis of a novel PEMFC-ORC combined power system. *Energy Conver Manag 217* 112998 (2020) **DOI:10.1016/j.enconman.2020.112998**.

[7] Wilberforce, T., Muhammad, I. Dynamic modelling and analysis of Organic Rankine Cycle power units for the recovery of waste heat from 110kW Proton Exchange Membrane Fuel cell system. *Int J Thermofl 17* 100280 (2023) **DOI:10.1016/j.ijft.2023.100280**.

[8] du Toit, L. Strengthening the global regulation of hydrofluorocarbons under the Montreal Protocol. *Reducing Emissions of Short-Lived Climate Pollutants Perspectives on Law and Governance Series: International Environmental Law,* 20 (2023) **DOI:10.1163/9789004684089_006**.

[9] Yang, M.H., Liu, M.C., Yeh, R.H. Investigation of low-GWP working fluids as substitutes for R245fa in organic Rankine cycle application. *Heliyon 10* (2024). **DOI:10.1016/j.heliyon.2024.e34219**.

[10] Elbir, A. Environmental impacts of F-gases and trifluoroacetic acid: Potential threats to aquatic ecosystems and management strategies. *Environ Progr Sust Energy 44* (2025) **DOI:10.1002/ep.70040**.

[11] Hafner, A. The advantages of natural working fluids. *Refrig Sci Techol 2019* 2456-2464 (2019) **DOI:10.18462/iir.icr.2019.1030**.

[12] Ibrahim, O.A.A.M., Kadhim, S.A., Hammoodi, K.A., Ashour, A.M., Bouabidi, A., Rashid, F.L., et al. Hydrocarbon refrigerants as sustainable alternatives to high-GWP refrigerants: a systematic review of R600 and R600a. *J Therm Analys Calorim 150* 17185-17206 (2025) **DOI:10.1007/s10973-025-14831-3**.

[13] Valiakina, A.V., Dolya, V.V. Review of experimental studies on the properties of the ozone-safe refrigerant R1234yf and their mathematical modeling using equations of state. *Refrig Technol 110* 193-204 (2021) **DOI:10.17816/RF626383**.

[14] Kuwar, Y.V. Performance evaluation of VCR system with pure and various blends of R134a, R1234yf, and R1234ze (E) refrigerants. *Heat Transf 53* 2879-2904 (2024) **DOI:10.1002/htj.23065**.

[15] Leto, A., Di Lorenzo, G. Development of a design tool for performance estimation and validation proton exchange membrane fuel cell: Verification and validation for 20 KW commercial fuel cell. *Fuels 5* 533-547 (2024) **DOI:10.3390/fuels5030029**.

[16] Sumeshan, S., Kumar, D.R., Krishna, B. Simulink model of proton exchange membrane fuel cell. *7th Int Conf Environ Friendly Energ Appl* (2022) 1-4, **DOI:10.1109/EFEA56675.2022.10063799**.

[17] Lu, C., Zhang, Y., Wang, X. Solubility Measurements of R1234ze (E), R1243zf, and R1234yf in POE46 at temperatures from 283.15 to 343.15 K. *J Chem Eng Data* 69 1677-1684 (2024) **DOI:10.1021/acs.jced.4c00022**.

[18] Nosrati-Ghods, N., Naidoo, M., Harrison, S.T.L., Isafiade, A.J., Tai, S.L. Embedding aspen custom modeller for bioethanol fermentation into the aspen plus flowsheet simulator. *Chem Eng Trans 80* 289-294 (2020) **DOI:10.3303/CET2080049**.

[19] Shalaby, S.M., Gadalla, M.A., El Sayed, A.R., Meliha, E.M., Abosheiasha, H.F. Aspen plus simulation of a low capacity organic Rankine cycle heated by solar energy. *Energy Rep 8* 416-421 (2022) **DOI:10.1016/j.egyr.2021.11.109**.

[20] Debtera, B., Ramesh, R., Neme, I., Ramesh, K., Murali, A. Fluidized bedreactor modeling and simulation with aspen plus for alumina (Al2O3) production systems. *Euro J Molec Clinic Med 8* 2021 (2021).

[21] Yang, Q., Liu, X., Xiao, G., Zhang, Z. PEMFC semi-empirical model improvement by reconstructing concentration loss. *Energies 18* 1754 (2025) **DOI:10.3390/en18071754**.

[22] Lee, H., Ryu, B., Anh, D.P., Roh, G., Lee, S., Kang, H. Thermodynamic analysis and assessment of novel ORC- DEC integrated PEMFC system for liquid hydrogen fueled ship application. *Int J Hydro Energ 48* 3135-3153 (2023) **DOI:10.1016/j.ijhydene.2022.10.135**.

[23] Lu, X., Du, B., Zhu, W., Yang, Y., Xie, C., Tu, Z., et al. Thermodynamic and dynamic analysis of a hybrid PEMFC-ORC combined heat and power (CHP) system. *Energ Conver Manag 292* 117408 (2023) **DOI:10.1016/j.enconman.2023.117408**.

[24] Kang, H.S., Kim, M.H., Shin. Y.H. Thermodynamic modeling and performance analysis of a combined power generation system based on HT-PEMFC and ORC. *Energies 13* 6163 (2020) **DOI:10.3390/en13236163**.

[25] Moon, J., Lee, H., Kim, H., Ji, H. Comparison of 50 kW ocean thermal energy conversion cycle performance by working fluid for marshall island application. *J Korea Soc Marin Env Energ 27* 229-237 (2024) **DOI:10.7846/JKOSMEE.2024.27.4.229**.

[26] Icaranom, J., Bolo, W.F., Yap, K.J., De Leon, R. On the viability of hydrofluoroolefin-R245fa mixtures as organic working fluids in a low-temperature solar-powered organic Rankine cycle (ORC). *IOP Conf Ser Mater Sci Eng 1318* 012054 (2024) **DOI:10.1088/1757-899X/1318/1/012054**.

[27] Witanowski, Ł. Multi-objective optimization of a small-scale ORC-VCC system using low-GWP refrigerants. *Energies 17* 5381 (2024) **DOI:10.3390/en17215381**.

[28] Park, C.S., Back, M.C., Park, H. A simulation on performance characteristics of secondary loop system for an electric vehicle with low gwp refrigerants. *Asia-Pacif J Converg Res Interch 10* 23-32 (2024) **DOI:10.47116/apjcri.2024.09.03**.

[29] Bull, J., Pound, J., Radulovic, J., Buick, J.M. Low-temperature ORC systems: Influence of the approach point and pinch point temperature differences. *Energies 18* 2954 (2025) **DOI:10.3390/en18112954**.

[30] Santana, J., Espinoza-Andaluz, M., Li, T., Andersson, M. A detailed analysis of internal resistance of a PEFC comparing high and low humidification of the reactant gases. *Front Energ Res 8* 572333 (2020) **DOI:10.3389/fenrg.2020.00217**.

[31] Li, S., Zhang, L., Chen, G., Zhang, R., Liu, A., Yang, G., et al. An experimental study on the performance of proton exchange membrane fuel cells with marine ion contamination. *J Mar Sci Eng 13* 1182 (2025) **DOI:10.3390/jmse13061182**.

[32] Salhi, I., Sadni, F.e., Belhora, F., Hajjaji, A. Thermodynamic analysis of basic and regenerative organic Rankine cycle configurations using six working fluids: A parametric study with coolprop in MATLAB. *J Ener Res Technol-A Sustain Renew Ener 1* 042101 (2025) **DOI:10.1115/1.4067544**.

[33] Hai, T., Ali, M.A., Alizadeh, A.ad., Almojil, S.F., Sharma, A., Almohana, Al., et al. Environmental analysis and optimization of fuel cells integrated with organic Rankine cycle using zeotropic mixture. *Int J Hydrog Energ 51* 1181-1194 (2024) **DOI:10.1016/j.ijhydene.2023.01.340**.

[34] Fan, L., Liu, Y., Luo, X., Tu, Z., Chan, S.H. Comparison and evaluation of mega watts proton exchange membrane fuel cell combined heat and power system under different waste heat recovery methods. *Renew Ener 210* 295-305 (2023) **DOI:10.1016/j.renene.2023.04.054**.

[35] Ngangué, M.N., Lekané, N.N., Njock, J.P., Sosso, O.T., Stouffs. P. Working fluid selection for a high efficiency integrated power/cooling system combining an organic Rankine cycle and vapor compression-absorption cycles. *Energy 277* 127709 (2023) **DOI:10.1016/j.energy.2023.127709**.

[36] Di, J., He, Q. Modeling and influencing factors analysis of proton exchange membrane fuel cell system coupled organic Rankine cycle under fixed output. *SSRN* 4617754 (2023) **DOI:10.2139/ssrn.4617754**

Acknowledgments *The authors would like to thank the Department of Mechanical and Industrial Engineering, Universitas Gadjah Mada, for providing the facilities and resources that made this research possible.*

Received *2026-02-04,* **revised** *2026-05-15,* **accepted** *2026-07-07 as original scientific paper.*

Data Availability *The data that support the findings of this study are available from the corresponding author upon reasonable request.*

Author Contribution *Bagus Putra Pratama: Conceptualization, Methodology, Software, Validation, Formal analysis, Investigation, Writing – Original Draft. Reynolds Widhiyanurrochmansyach: Formal Analysis, Methodology, Visualization, Investigation, Writing – Review & Editing. Jayan Sentanuhady: Supervision, Conceptualization, Writing – Review & Editing, Project administration, Funding acquisition. Widya Wijayanti: Writing – Review & Editing.*

AI Assisted Writing *During the preparation of this manuscript, the authors utilized several generative AI tools to assist in various stages of the research and writing process. Specifically, ChatGPT and Gemini were used for improving language, clarity, and grammatical structure. Scispace and Elicit were employed for literature searching and summarizing relevant research articles. BioRender was used to create the graphical abstract and other schematic figures. QuillBot was utilized for paraphrasing and refining sentence structures. Following the use of these tools, the authors meticulously reviewed and edited the entire manuscript and assume full responsibility for the final content of this publication.*

Izboljšanje učinkovitosti gorivne celice PEM z integriranim organskim Rankinovim ciklom z uporabo delovnih fluidov z nizkim potencialom globalnega segrevanja

Povzetek *Gorivne celice s protonsko izmenjevalno membrano (PEMFC) omogočajo visoko učinkovito proizvodnjo električne energije brez emisij, vendar se od 45 % do 60 % njihove vhodne kemijske energije izgubi v obliki nizkotemperaturne odpadne toplote. Za reševanje tega problema je v raziskavi predstavljena termodinamična analiza 50-kW gorivne celice PEMFC, toplotno integrirane s podkritičnim organskim Rankinovim ciklom (ORC), ki omogoča pretvorbo te odpadne toplote v dodatno električno moč. Z uporabo natančnega modela validiranega s prejšnjo študijo, so delovni fluidi z nizkim potencialom globalnega segrevanja (GWP) (R1233zd(E), R1234yf in R1234ze(Z)) primerjani s tradicionalnim fluidom R245fa ob uporabi praktične strategije regulacije s fiksnimi točkami stanji. Rezultati kažejo do 3-odstotno povečanje skupnega električnega izkoristka zaradi uspešne pretvorbe nizkotemperaturne odpadne toplote gorivne celice PEMFC v dodatno neto moč v spodnjem ciklu ORC. Glavna novost raziskave je prva celovita potrditev, da je mogoče z uporabo delovnih fluidov z nizkim GWP in praktične strategije regulacije s fiksnimi stanji trajnostno doseči 3-odstotno izboljšanje izkoristka celotnega sistema ter hkrati zagotoviti stabilno obratovanje. Analiza potrjuje, da je mogoče doseči termodinamično omejen 5-odstotni toplotni izkoristek ORC brez zmanjšanja potenciala za rekuperacijo energije, kar dokazuje, da je mogoče zahteve po trajnosti združiti z izboljšanjem zmogljivosti sistema. R1234yf se je izkazal kot najprimernejši fluid z nizkim GWP pri obratovanju z visokimi obremenitvami, medtem ko je R1233zd(E) optimalen pri nizkih obremenitvah, kar potrjuje zanesljiv pristop k načrtovanju okolju prijaznih sistemov gorivnih celic naslednje generacije.*

Ključne besede *gorivna celica s protonsko izmenjevalno membrano, organski Rankinov cikel, delovni fluid z nizkim potencialom globalnega segrevanja, izraba odpadne toplote*